Academic Journal of Science and Technology
ISSN: 2771-3032 | Vol. 20, No. 1, 2026

Construction of Micro-crumpled Nanofiltration Membranes based on Metal Organic Frameworks Interlayers and Their Efficacy in Water Treatment

Peiyao Wang [1], Ping Li [2], Chengling Bai [1], Xitong Wang [1], Shuili Yu [1, 3, *]

[1] State Key Laboratory of Pollution Control and Resources Reuse, College of Environmental Science and Engineering, Tongji University, Shanghai, 200092, China
[2] Innovation Center of Yangtze River Delta, Zhejiang University, Jiaxing Zhejiang, 314100, China
[3] Shanghai Institute of Pollution Control and Ecology Safety, Shanghai 200092, China

*** Corresponding author:** Shuili Yu

Abstract: Surface chemistry, morphology, and network architecture jointly of nanofiltration (NF) membranes significantly influence their water treatment performance. Within these levers, constructing micro-crumpled polyamide (PA) skins has emerged as a promising tactic to simultaneously enhance permeability, selectivity, and fouling resistance. Based on this, the strategy of introducing metal-organic framework (MOFs) materials as an intermediate layer to construct micro-crumpled structures offers a novel approach to addressing the traditional trade-off between permeability and selectivity in nanofiltration membranes. However, the strategies, mechanisms, and effects of using MOF intermediate layers have not yet been systematically summarized. This paper explores the influencing factors in preparing micro-crumpled nanofiltration membranes based on MOFs interlayers. It reviews different preparation methods and their mechanisms, focusing on how the nature and introduction mode of MOFs affect the micro-crumpled structure and modulation mechanism. Additionally, it examines the influence of the micro-crumpled selective layer on the permeability, selectivity, and anti-contamination performance of nanofiltration membranes. Finally, it outlines the current research shortcomings and envisions future research directions and objectives for using MOFs interlayers to construct micro-crumpled nanofiltration membranes.

Keywords: Water Treatment; Nanofiltration; Micro-Crumpled; Metal-Organic Frameworks (MOFs); Interfacial Polymerization.

1. Introduction

Nanofiltration membranes, as an emerging water purification technology, offer advantages such as low energy consumption and high separation efficiency and have been deployed in wastewater reclamation, seawater purification, and high-quality drinking water production [1–4]. The mainstream NF membranes architecture is the thin-film composite (TFC) membrane, in which a polyamide (PA) selective layer is formed on a porous polymer substrate via interfacial polymerization (IP) between piperazine (PIP) and trimesoyl chloride (TMC). In recent years, micro-crumpled NF membranes have attracted increasing attention owing to their distinctive surface morphology, high water permeance, and, to some extent, improved solute rejection [5]. Earlier studies on micro-crumpled membranes primarily focused on tuning monomer concentrations [6–7], introducing additives [8], employing substrate templating [9], or utilizing nanofoaming strategies [10]. However, performance gains through monomer tuning or additive introduction are often limited; substrate templating can incur a risk of support-pore blockage, thereby reducing permeability [11]; nanofoaming may suffer from bubble escape, impose stringent requirements on the substrate, and lead to collapse of nano-void structures during drying, adversely affecting permeability [12].

By contrast, introducing porous nanomaterials as an interlayer template atop the support offers a fabrication strategy that simultaneously regulates IP, introduces additional water transport pathways, mitigates permeability loss, and preserves structural stability [13]. Porous nanomaterials commonly used as interlayers fall into two classes: inorganic (e.g., carbon nanotubes [14], silver nanowires [15], cellulose nanofibers [16], graphene oxide (GO) [17]) and organic (e.g., metal–organic frameworks (MOFs) [18], covalent organic frameworks (COFs) [19]). Among them, MOFs—owing to their high specific surface area, ordered porosity, and multifunctionality—have been widely employed as interlayers. By tailoring MOF particle size, morphology, deposition density, and surface functional groups, the membrane surface topography can be effectively engineered [20–22]. Moreover, the mode of MOF introduction (e.g., pre-loaded IP versus blended IP) exerts a decisive influence on membrane performance [23]. This article reviews preparation methods and formation mechanisms of MOF-interlayer-enabled micro-crumpled NF membranes, and summarizes advances linking morphology evolution to NF performance.

2. Overview of Micro-Crumpled Membranes

2.1. Definition

Conventional TFC membranes prepared from PIP and TMC exhibit smooth, flat PA layers at low PIP concentrations. In comparison, micro-crumpled NF membranes refer to PA composite membranes whose selective layers display nanometer-scale crumpled morphologies [24].

2.2. Characteristics

Depending on their morphological motifs, micro-crumpled membranes are typically categorized as nodular, ring-like, ridge-like, or thin-layer folded [25]. Due to their pronounced surface undulations and higher roughness (RMS roughness: 30–100 nm), these membranes have a larger effective surface area. This enables a greater area of contact with water to be developed over a limited perimeter [26]. In addition, micro-crumpled membranes often possess higher porosity and auxiliary water transport channels, enabling high permeability whilst maintaining desirable selectivity [27].

3. Micro-Crumpled Membranes Based on MOF Interlayers

In recent years, depositing MOFs on the support surface to construct thin-film nanocomposite (TFN) membranes has reduced the risk of support-pore blockage and enhanced structural robustness. The interlayer can modulate surface chemistry and enrich monomers near the reaction front. As a template, it enlarges the contact area between the aqueous and organic phase, provides more complex monomer diffusion pathways, and promotes the development of non-uniform monomer concentration fields at the interface. These effects amplify crumpling on the rugged interlayer template [13]. The resultant PA morphology, however, depends strongly on the intrinsic properties of the MOFs and their introduction routes.

3.1. Effects of MOF Properties on Micro-Crumpled

(1) Physicochemical properties

MOFs of different sizes and architectures induce distinct crumpled morphologies. In general, smaller particles favor more uniform crumple distributions, whereas larger particles tend to generate more pronounced crumples but with an elevated defect risk [28]. Xiao et al. [29] showed that amino-functionalized MOFs of varying sizes (300, 400, and 800 nm) induced different crumple types: small MOF particles were readily embedded in the PA layer forming nodular protrusions with a low defect probability, while increasing particle size enhanced ridge-like features with wider ridges and yielded a higher degree of PA crosslinking.

MOFs with three-dimensional architectures more readily produce ridge–valley topographies, whereas rod-like MOFs tend to form ring-like or sheet-like folds [30]. For example, MOF-808, which appears as spherical agglomerates of regular hexahedra, predominantly yields nodular TFN surfaces and can form ring-like or sheet-stacked structures under specific conditions [31]; by contrast, MIL-101(Cr)–NH_2, an octahedral, vertex-sharing super-tetrahedral MOF with comparable particle size and loading, gives rise to ridge–valley morphologies [32]. Ultrathin 2D-MOF nanosheets prepared by ultrasonic exfoliation, when used as interlayers, afford ring-type crumples at low loadings and sheet-stacked folds at high loadings [33]. Rod-like PCN-222 with an aspect ratio of ~3 can induce ridge–valley features even at relatively low loadings [34]. Related studies using nanomaterials with different shapes further corroborate the correlation between MOF morphology and TFN crumpling behavior [35].

Different functional groups endow MOFs with distinct physicochemical properties. Oxygen-containing moieties (e.g., hydroxyl, carboxyl, sulfonic groups) can strengthen electrostatic and hydrogen-bonding interactions with PIP, thereby regulating the IP process to generate crumples and improve permeation. Lin et al. [36] demonstrated that UiO-66-NH_2@PA exhibited more extensive crumpling, elevated surface roughness and increased water permeance (6.7 L m^{-2} h^{-1} bar^{-1}), which is approximately 1.4 times higher than that of UiO-66@PA. In addition to influencing the distribution and diffusion of PIP, MOF functional groups often interact with PA oligomers, thereby affecting PA formation [37].

(2) Deposition density

Deposition density is defined as the mass of the MOF per unit area of the interlayer. Numerous studies have examined the morphological changes that occur at different deposition densities. At high densities, crumple features become more pronounced. However, excessive loading increases agglomeration and the risk of defects. At low densities, crumples are smaller, more densely distributed and more uniform, yielding thinner PA with relatively lower roughness. Wang et al. [20] systematically studied the effects of nanoparticle size and loading on micro-crumpling and found that increasing the deposition density from 0.9 to 6.4 μg·cm^{-2} progressively intensified the crumpling. An optimum deposition density of 4.3 μg·cm^{-2} delivered the best combined performance in terms of water permeance (53.5 L m^{-2} h^{-1} bar^{-1}) and Na_2SO_4 rejection (95%).

3.2. Effects of MOF Introduction Route on Micro-crumpled

Multiple factors influence TFN crumpling. Even MOFs bearing identical functional groups can yield different crumple patterns depending on the introduction route [38].

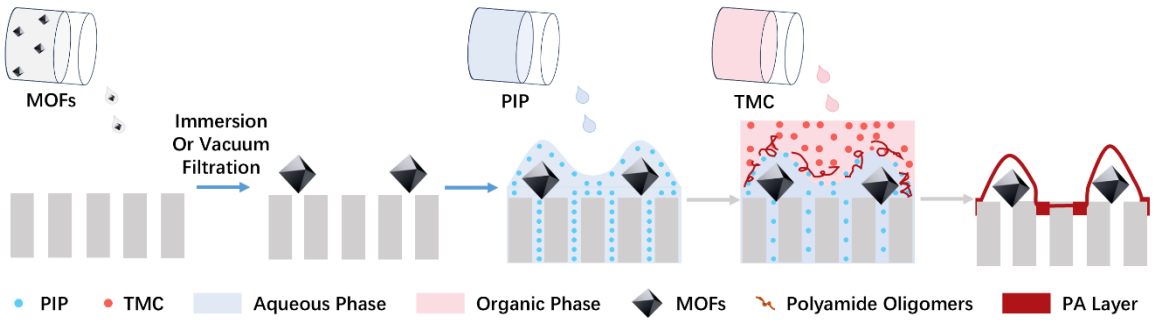


Fig 1. Schematic of the pre-loaded interfacial polymerization method.

(1) Pre-loaded interfacial polymerization

In this approach, MOFs are first distributed onto the substrate via immersion or vacuum filtration to form an interlayer, followed by IP on top. The immersion method is straightforward: submerging the substrate in a MOF suspension allows physiosorbed MOFs to form an interlayer.

However, weak interfacial adhesion can lead to MOF migration or shedding, resulting in a significant decrease in performance under sustained pressure or hydrodynamic scouring [39]. In contrast, vacuum filtration/pressure-assisted deposition places MOFs uniformly on the porous substrate surface before IP. This reduces MOF displacement and consumption while strengthening interfacial adhesion. Consequently, mechanical robustness and service life are improved [40]. Although the influence of pre-loaded MOFs on PA crosslinking is limited, the deposited particles augment substrate roughness and facilitate the formation of a more crumpled PA layer [30].

(2) Blended interfacial polymerization

Unlike directly depositing MOFs from an aqueous suspension, blended IP mixes MOFs with other components prior to introduction onto the substrate, typically via stirring or ultrasonication.

Blended IP can be divided into aqueous phase blending and additive blending. In aqueous phase blending, the aqueous monomer is co-mixed with MOFs and delivered during IP. In additive blending, MOFs are co-mixed with selected additives prior to deposition, and the mixture is pressure-filtered onto the substrate to form the interlayer.

During aqueous phase blending, additional steps to remove and air-knife excess aqueous solution can cause greater MOF loss than in pre-loaded IP, leading to lower-than-expected MOF loading and, consequently, fewer and less uniform crumples. If pressure assistance (vacuum or positive pressure) is applied to filter the MOF–PIP dispersion onto the substrate, the removal steps can be minimized, reducing MOF loss; the one-step filtration also curtails particle migration, achieving a more uniform interlayer [38]. Jointly, these effects not only promote crumple formation but also yield richer and more homogeneous crumple patterns. Using PIP aqueous phase blending, Li et al. [37] observed striped crumples on the membrane surface, with MOFs encapsulated beneath the PA layer; substantial thickness differences between MOF-surrounding regions and smooth cross-sections indicate that PIP aqueous phase blending is advantageous for generating more complex surface structures.

Additive blending offers further levers. Co-mixing strongly hydrophilic additives promotes water microphase clustering and increases MOF adsorption of amine monomers, elevating the local aminoacyl chloride ratio and favoring highly crosslinked PA; co-mixing hydrogen-bond-forming additives with PIP slows PIP diffusion, leading to dense, striped crumples [41–43]. Conversely, strongly anionic additives can markedly raise the amine monomer concentration at the interface, intensify IP, and generate a denser nascent PA prone to earlier self-limiting growth [44]. The combined effects of retarded PIP diffusion and enhanced self-limitation restrict PA growth, promoting relatively thin, folded-sheet PA layers.

In our group's study, we investigated MOF co-blending with different additive classes: MOF–hydroxyl co-blends yielded an average surface roughness of 22.0 nm with high-density striped crumples, whereas MOF co-blends with negatively charged species produced a roughness of 78.0 nm with larger crumples and a relatively thin, folded-sheet morphology.

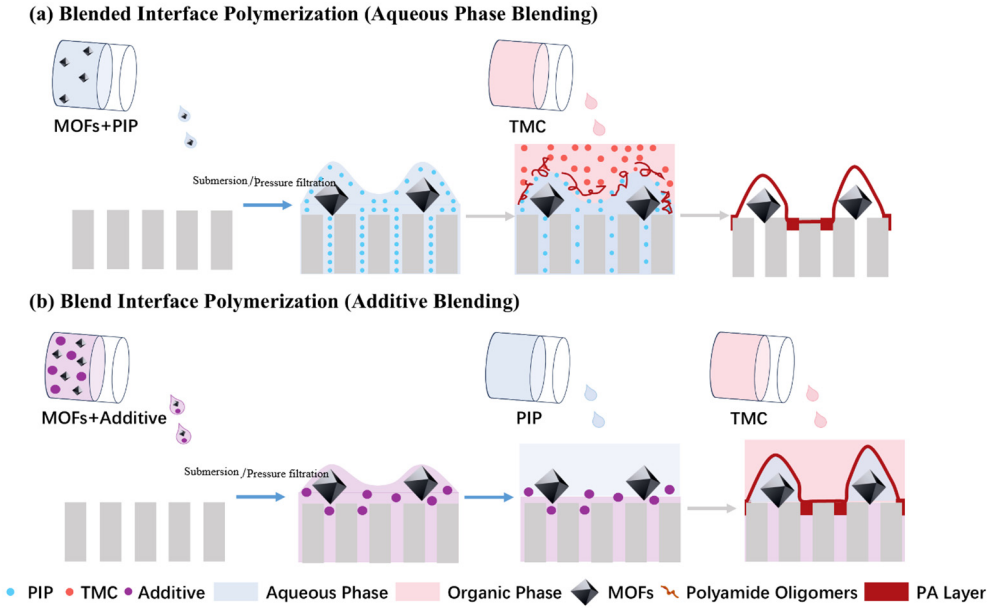


Fig 2. Schematic Diagram of Blended Interfacial Polymerization

4. Water-Treatment Performance

4.1. Permeation

Micro-crumpled membranes generally exhibit higher permeation than TFC controls, attributable to the increased effective water-contactable area imparted by crumpling and to additional transport channels arising from the MOF interlayer.

(1) Effective area

Water permeation is primarily governed by a diffusion mechanism. The MOF interlayer renders a distinctive crumpled architecture that increases surface area and thereby the amount of water diffusing through the membrane, enhancing permeance. The enlarged surface area often acts synergistically with a reduced PA thickness, which lowers mass-transfer resistance; larger crumples commonly coincide with thinner PA, both favoring water transport. Shakiba et al. [45] dispersed MIL-53(Al) in the organic phase as an interlayer template and increased the average surface

roughness of the TFN0.5 membrane to 78.27 nm (versus 38.84 nm for TFC). The higher roughness delivered a larger specific area and improved hydrophilicity, and the TFN0.5 permeance reached 2.7 ± 0.19 L m^{-2} h^{-1} bar^{-1}. In another system with MOF-235 participation, PA thickness decreased from 104 nm to 50 nm while surface area increased from 28.1 μm^2 to 39.9 μm^2, resulting in an approximately five-fold flux increase compared with TFC [46].

(2) Additional channels

The interlayer lowers transport resistance by thinning the PA layer and providing auxiliary pathways, thereby further improving permeance [47]. In MOF-interlayered crumpled membranes, water flows not only through the PA free-volume network but also via intracrystalline MOF pores and MOF–PA interfacial corridors that can connect longitudinally, producing a "trench effect" that markedly shortens the transport pathlength and enhances efficiency [48]. Jiang et al. [49] reported significantly increased permeance for TFN membranes relative to TFC counterparts without MIL-101/Fe_3O_4; the improvement was primarily attributed to the porosity of MIL-101/Fe_3O_4 and the presence of the interlayer, which provided additional water pathways.

4.2. Rejection Performance

As noted, micro-crumpled membranes are highly permeable and are subject to the classical permeability–selectivity trade-off. Nevertheless, for MOF-interlayered micro-crumpled membranes, enhancements in permeation typically arise from multiple, coupled mechanisms, enabling them to maintain salt rejection comparable to TFC membranes and thereby approach a higher permeability–selectivity upper bound. Additionally, intrinsic interlayer properties—such as hydrophilicity and surface charge—exert a pivotal influence on ion sieving and solute separation.

(1) Structural optimization

The interlayer can optimize the PA structure, rendering it denser and defect-free, which enhances salt rejection. As described in §2.2, MOF interlayers enrich PIP at the reaction front, increasing the local PIP concentration and PA crosslinking. Cheng et al. [13] prepared TFN membranes with MOF interlayers on various substrates and found reduced molecular-weight cut-offs relative to TFC controls; except for TFN150, TFN membranes exhibited higher PA crosslinking than TFC. Moreover, TFN membranes with interlayers achieved sulfate (SO_4^{2-}) rejections comparable to commercial NF270, with TFN300 reaching ≥97% SO_4^{2-} rejection.

(2) Charge regulation

The charge of the MOF interlayer can strengthen Donnan exclusion, improving selectivity toward specific ions. Hetero-charged interlayers can also regulate the structure of the selective PA layer by altering PIP diffusion to the interface, while their own charge directly modulates the rejection behavior of the resulting TFC. For example, employing negatively charged UiO-66-NO_2 as an interlayer yielded a zeta potential of −26.1 mV at pH 7, significantly enhancing electrostatic repulsion toward SO_4^{2-}. Li et al. [37] reported that membranes with UiO-66-NO_2 interlayers—owing to smaller mean pore size, a narrower pore-size distribution, and stronger negative surface charge—achieved high rejections for salts with divalent anions and divalent cations (Na_2SO_4: 99.1%, $MgCl_2$: 95.5%).

In assessing rejection, mixed-salt performance is equally important. Unlike single-salt systems, mixed-salt solutions require consideration of both membrane–ion and ion–ion interactions. Thus, NF selectivity is governed not only by membrane parameters (pore size, surface charge) but also by ion parameters (hydrated size, valence). In general, reducing pore size and enhancing negative surface charge favor selective rejection of Cl^- and SO_4^{2-}; conversely, reducing pore size and enhancing positive charge favor selective rejection of Mg^{2+} and Na^+. Besides size-tunable pores, MOFs offer abundant organic ligands capable of selectively repelling specific ions via electrostatic or chemical interactions, thus improving ion-type selectivity. Using lysine-modified UiO-66 (Lys@UiO-66) as the interlayer, the TFN-LDU8 membrane achieved excellent monovalent/divalent ion selectivity (separation factor 42.27) due to the combined effects of positive charge and small pore size [48].

4.3. Antifouling Performance

(1) Fouling risk

Surface morphology is a key determinant of fouling. Generally, smooth and highly hydrophilic membranes exhibit lower fouling propensity, whereas highly crumpled and rough surfaces can promote contaminant adsorption and accumulation, create local dead zones, and thereby elevate fouling risk. The angle between crumple orientation and bulk flow can also modulate fouling behavior [50]. Importantly, crumpling and fouling risk are not strictly positively correlated. When the characteristic foulant size is comparable to the inter-ridge spacing, fouling risk is high; when foulants are much smaller or much larger than the spacing, fouling risk diminishes. Shang et al. [51] investigated fouling for membranes with distinct crumple morphologies. An enhanced nano-crumpled membrane (E-NF) prepared by adding 6 wt% $NaHCO_3$ during IP possessed larger ridge–valley spacing, exhibited lower foulant attachment and easier cleaning, and—owing to its larger overall water-contactable area—retained appreciable permeance after extended operation.

(2) Antifouling properties

Chemical properties (charge, hydrophilicity) also affect fouling. MOFs can be tailored—by selecting charged/hydrophilic ligands or through post-synthetic modification (e.g., grafting zwitterionic polymers)—to increase interlayer hydrophilicity, enhance surface repulsion of foulants, or weaken attractive interactions, thereby improving antifouling. Furthermore, antibacterial MOFs (e.g., Ag-MOF) can inactivate bacteria adhering to the membrane surface and effectively mitigate biofouling. Seyedpour et al. [52] prepared TFN membranes with an Ag-MOF interlayer, which enhanced hydrophilicity and negative charge. Compared with TFC, the water contact angle decreased from 72.6 ± 5.1° to 43.4 ± 3.1°. Against *E. coli* as a model Gram-negative bacterium, the viable cell count on Ag-MOF-TFN surfaces decreased by >92% relative to TFC, evidencing significant antibacterial performance.

5. Conclusion

(1) Influence of MOF properties on membrane characteristics. Small MOFs favor uniform nodular morphologies; larger and three-dimensional MOFs tend to form ridge–valley structures; plate-/rod-like MOFs incline toward ring-/sheet-like crumples. There exists an optimal deposition density: overly low density leads to small, densely distributed crumples, thin PA, and lower roughness; overly high density yields pronounced crumples but increases agglomeration and defect risks. Additionally, amino-functionalized (and other tailored) MOFs can enhance

hydrophilicity and monomer interactions, thereby optimizing PA crosslinking and controlled roughness.

(2) Influence of MOF introduction route on membrane characteristics. Vacuum-filtered pre-loaded IP enables uniform and robust MOF dispersion and promotes formation of crumpled PA layers. Blended IP exhibits route-specific features: aqueous phase blending without pressure assistance tends to incur MOF loss and irregular crumpling (pressure assistance is required to improve loading uniformity); additive blending can regulate monomer diffusion and reaction kinetics, inducing highly crosslinked striped crumples (with hydrophilic additives) or thin folded-sheet morphologies (with strongly anionic additives).

Through the coordinated control of these factors, NF performance can be systematically optimized:

Introducing a MOF interlayer can increase water permeance by approximately five-fold relative to conventional TFC membranes.

Precise control over pore size, pore-size distribution, and surface charge via the interlayer enables simultaneously high rejections for salts containing divalent anions and divalent cations (e.g., Na_2SO_4: 99.1%, $MgCl_2$: 95.5%).

With antibacterial interlayers, viable bacterial counts on TFN surfaces can be reduced by >92% versus TFC, substantially mitigating fouling.

In summary, incorporating MOF interlayers offers a novel and practical pathway toward high-performance NF membranes. Notwithstanding significant progress, challenges remain, suggesting the following priorities for future research:

The regulatory mechanisms by which MOFs influence IP kinetics are not yet fully elucidated, and quantitative relationships linking crumple morphology to membrane performance are lacking. Future work should combine molecular dynamics with machine learning to establish predictive structure–kinetics–performance models ("MOF structure–IP dynamics–membrane performance") to guide materials design and optimization.

Although MOFs enhance water-treatment efficacy, their long-term stability and applicability in complex waters require further verification. The synergistic effects of MOF combinations and integration with other membrane design/modification strategies should also be explored to achieve more efficient water treatment.

Acknowledgments

The authors gratefully acknowledge the financial support from the National Natural Science Foundation of China (Grant numbers: 52170011).

References

[1] Maroufi N, Hajilary N. Nanofiltration membranes types and application in water treatment: a review [J]. Sustainable Water Resources Management, 2023, 9(5): 142.

[2] Al Harby N F, El-Batouti M, Elewa M M. Prospects of polymeric nanocomposite membranes for water purification and scalability and their health and environmental impacts: a review [J]. Nanomaterials, 2022, 12(20): 3637.

[3] Bassyouni M, Abdel-Aziz M H, Zoromba M S, et al. A review of polymeric nanocomposite membranes for water purification [J]. Journal of Industrial and Engineering Chemistry, 2019, 73: 19-46.

[4] Guo Hao, Li Xianhui, Yang Wulin, et al. Nanofiltration for drinking water treatment: a review [J]. Frontiers of Chemical Science and Engineering, 2022, 16(5): 681-698.

[5] Tan Zhe, Chen Shengfu, Peng Xinsheng et al. Polyamide membranes with nanoscale turing structures for water purification [J]. Science, 2018, 360(6388): 518-521.

[6] Nulens I, Peters R, Verbeke R, et al. MPD and TMC supply as parameters to describe synthesis-morphology-performance relationships of polyamide thin film composite membranes [J]. Journal of Membrane Science, 2023, 667: 121155.

[7] Gan Qimao, Peng L E, Yang Zhe, et al. Demystifying the role of surfactant in tailoring polyamide morphology for enhanced reverse osmosis performance: mechanistic insights and environmental implications [J]. Environmental Science & Technology, 2023, 57(4): 1819-1827.

[8] Tang Jingwen, Bai Chengling, Yu, Shuili, et al. Aqueous phase co-solvent-assisted preparation of high-performance polyamide nanofiltration membranes: preparation, performance and mechanistic [J]. Surfaces and Interfaces, 2025, 62: 106168.

[9] Peng L E, Yang Zhe, Long Li, et al. A critical review on porous substrates of TFC polyamide membranes: Mechanisms, membrane performances, and future perspectives [J]. Journal of Membrane Science, 2022, 641: 119871.

[10] Ma Xiaohua, Yao Zhikan, Yang Zhe, et al. Nanofoaming of polyamide desalination membranes to tune permeability and selectivity [J]. Environmental Science & Technology Letters, 2018, 5(2): 123-130.

[11] Zhang Ruijun, Yu Shuili, Shi Wenxin, et al. Support membrane pore blockage (SMPB): an important phenomenon during the fabrication of thin film composite membrane via interfacial polymerization [J]. Separation and Purification Technology, 2019, 215: 670-680.

[12] Gan Qimao, Hu Yaowen, Wu Chenyue, et al. Nanofoamed Polyamide Membranes: Mechanisms, Developments, and Environmental Implications [J]. Environmental Science & Technology, 2024, 58(47): 20812-20829.

[13] Cheng Peng, Liu Yanling, Wei Xinxin, et al. Distinct Efficacies of Interlayers in Tailoring Polyamide Nanofiltration Membrane Performance for Organic Micropollutant Removal: Dependent on Substrate Characteristics [J]. Environmental Science & Technology, 2024, 58(31): 14022-14033.

[14] Ma Xiaohua, Guo Hao, Yang Zhe, et al. Carbon nanotubes enhance permeability of ultrathin polyamide rejection layers [J]. Journal of Membrane Science, 2019, 570-571: 139-145.

[15] Jackson J C, Camargos C H M, Liu Caihong, et al. Antimicrobial activity of thin-film composite membranes functionalized with cellulose nanocrystals and silver nanoparticles via one-pot deposition and layer-by-layer assembly [J]. Environmental Science: Water Research & Technology, 2024, 10(3): 639-651.

[16] Cruz-Silva R, Izu K, Maeda J, et al. Nanocomposite desalination membranes made of aromatic polyamide with cellulose nanofibers: synthesis, performance, and water diffusion study [J]. Nanoscale, 2020, 12(38): 19628-19637.

[17] Lai G S, Lau W J, Goh P S, et al. Tailor-made thin film nanocomposite membrane incorporated with graphene oxide using novel interfacial polymerization technique for enhanced water separation [J]. Chemical Engineering Journal, 2018, 344: 524-534.

[18] Li Baoyin, You Xinda, Wu Hong, et al. A facile metal ion pre-anchored strategy for fabrication of defect-free MOF membranes on polymeric substrates [J]. Journal of Membrane Science, 2022, 650: 120419.

[19] Zhang Zhe, Shi Xiansong, Wang Rui, et al. Ultra-permeable polyamide membranes harvested by covalent organic framework nanofiber scaffolds: a two-in-one strategy [J]. Chemical Science, 2019, 10(39): 9077-9083.

[20] Wang Zhenyi, Wang Zhangxin, Lin Shihong, et al. Nanoparticle-templated nanofiltration membranes for ultrahigh performance desalination [J]. Nature Communications, 2018, 9(1): 2004.

[21] Le Tin, Chen Xi, Dong Hang, et al. An Evolving Insight into Metal Organic Framework-Functionalized Membranes for Water and Wastewater Treatment and Resource Recovery [J]. Industrial & Engineering Chemistry Research, 2021, 60(19): 6869-6907.

[22] Shi Lixiu, Shi Yahui, Xu Yaqing, et al. Metal-organic framework membranes with varying metal ions for enhanced water and wastewater treatment: A critical review [J]. Journal of Environmental Chemical Engineering, 2023, 11(6): 111468.

[23] Wu Xiaona, Yang Lei, Meng Fanbin, et al. ZIF-8-incorporated thin-film nanocomposite (TFN) nanofiltration membranes: Importance of particle deposition methods on structure and performance [J]. Journal of Membrane Science, 2021, 632: 119356.

[24] Shao Senlin, Zeng Fanxi, Long Li, et al. Nanofiltration Membranes with Crumpled Polyamide Films: A Critical Review on Mechanisms, Performances, and Environmental Applications [J]. Environmental Science & Technology, 2022, 56(18): 12811-12827.

[25] Shi Yongxuan, Wang Zheng, Mai Zhaohuan, et al. Nanomorphogenesis of template-induced crumpled polyamide nanofiltration membranes [J]. Journal of Membrane Science, 2023, 686: 121997.

[26] Nulens I, Ben Zvi A, Vankelecom I F J, et al. Re-thinking polyamide thin film formation: How does interfacial destabilization dictate film morphology? [J]. Journal of Membrane Science, 2022, 656: 120593.

[27] Yuan Bingbing, Zhang Yuhang, Qi Pengfei, et al. Self-assembled dendrimer polyamide nanofilms with enhanced effective pore area for ion separation [J]. Nature Communications, 2024, 15(1): 471.

[28] Wang Feihong, Zheng Tong, Xiong Ruohan, et al. Strong improvement of reverse osmosis polyamide membrane performance by addition of ZIF-8 nanoparticles: Effect of particle size and dispersion in selective layer [J]. Chemosphere, 2019, 233: 524-531.

[29] Xiao Shujuan, Huo Xiaowen, Fan Shuxin, et al. Design and synthesis of Al-MOF/PPSU mixed matrix membrane with pollution resistance [J]. Chinese Journal of Chemical Engineering, 2021, 29: 110-120.

[30] Zhao Yangying, Liu Yanling, Wang Xiaomao, et al. Impacts of Metal-Organic Frameworks on Structure and Performance of Polyamide Thin-Film Nanocomposite Membranes [J]. ACS Applied Materials & Interfaces, 2019, 11(14): 13724-13734.

[31] Zhao Zhenzhen, Wang Tao, Zheng Xi, et al. MOF-808/Polyamide Thin-Film Nanocomposite Membranes for Efficient Nanofiltration [J]. ACS Applied Nano Materials, 2023, 6(19): 17615–17625.

[32] Han Gang, Studer R M, Lee M, et al. Post-synthetic modification of MOFs to enhance interfacial compatibility and selectivity of thin-film nanocomposite (TFN) membranes for water purification [J]. Journal of Membrane Science, 2023, 666: 121133.

[33] Liu Yi, Wang Xinping, Zong Ziao, et al. Thin film nanocomposite membrane incorporated with 2D-MOF nanosheets for highly efficient reverse osmosis desalination [J]. Journal of Membrane Science, 2022, 653: 120520.

[34] Bonnett B L, Smith E D, Garza M D L, et al. PCN-222 Metal–Organic Framework Nanoparticles with Tunable Pore Size for Nanocomposite Reverse Osmosis Membranes [J]. ACS Applied Materials & Interfaces, 2020, 12(13): 15765–15773.

[35] Gao Xuerui, Li Ping, Gu Zhengyang, et al. Preparation of poly(piperazine-amide) nanofilms with micro-wrinkled surface via nanoparticle-templated interfacial polymerization: Performance and mechanism [J]. Journal of Membrane Science, 2021, 638: 119711.

[36] Lin Yuqing, Wu Haochen, Shen Qin, et al. Custom-tailoring metal-organic framework in thin-film nanocomposite nanofiltration membrane with enhanced internal polarity and amplified surface crosslinking for elevated separation property [J]. Desalination, 2020, 493: 114649.

[37] Li Ping, Gu Zhengyang, Bai Chengling, et al. Effects of MOFs size and functional group on the pore structure and performance of thin-film nanocomposite membranes [J]. Journal of Membrane Science, 2023, 686: 121979.

[38] Wan Chik, W. S., Goh, P. S., Xue, Qingquan, et al. Advancing Forward Osmosis Thin-Film Composite Membranes with Metal-Organic Framework: Strategies for Enhanced Performance and Efficiency [J]. Separation & Purification Reviews 2025: 1-18.

[39] Jia Yanjun, Huo Xiaowen, Gao Lu, et al. Controllable Design of Polyamide Composite Membrane Separation Layer Structures via Metal-Organic Frameworks: A Review [J]. Membranes (Basel), 2024, 14(9): 201.

[40] Zhao Dieling, Feng Fan, Shen Liguo, et al. Engineering metal–organic frameworks (MOFs) based thin-film nanocomposite (TFN) membranes for molecular separation [J]. Chem Eng J, 2023, 454: 140447.

[41] Ge Lei, Song Hengjie, Zhu Junyong, et al. Metal/covalent–organic framework based thin film nanocomposite membranes for advanced separations [J]. Journal of Materials Chemistry A, 2024, 12(14): 7975-8013.

[42] Zhang Saihui, Li Xiaoyang, Gao Hui, et al. Recent progress in additives in interfacial polymerization for the preparation of polyamide composite membrane [J]. Chemical Industry and Engineering Progress, 2022, 41(9): 4884-4894.

[43] He Miaolu, Li Yushuang, Feng Leihao, et al. Mechanism for regulation of a forward osmosis membrane by the SA/UiO-66-NH2 composite interlayer and the resulting lithium ion concentration performance [J]. Journal of Cleaner Production, 2023, 410: 137282.

[44] Huo Xiaowen, Jing Zhaojing, Wang Haitao, et al. Sodium dodecyl sulfate/C-UIO-66 regulation of nanofiltration membrane with pleated and thin polyamide layer structure [J]. Desalination, 2022, 538: 115927.

[45] Samsami S, Sarrafzadeh M-H, Ahmadi A. Surface modification of thin-film nanocomposite forward osmosis membrane with super-hydrophilic MIL-53 (Al) for doxycycline removal as an emerging contaminant and membrane antifouling property enhancement [J]. Chemical Engineering Journal, 2022, 431: 133469.

[46] Chen Jinchao, Bai Yong, Nabil Shokry Gadallah E, et al. Enhancing the perm-selectivity of thin-film nanocomposite membranes intercalated with cyclodextrin-chelated Metal-Organic Framework via modulated interfacial polymerization [J]. Journal of Membrane Science, 2024, 693: 122382.

[47] Sun Pengfei, Yang Zhe, Song Xiaoxiao, et al. Interlayered Forward Osmosis Membranes with Ti3C2Tx MXene and Carbon Nanotubes for Enhanced Municipal Wastewater Concentration [J]. Environmental Science & Technology, 2021, 55(19): 13219-13230.

[48] Gu Zhengyang, Yu Shuili, Zhu Junyong, et al. Incorporation of lysine-modified UiO-66 for the construction of thin-film nanocomposite nanofiltration membrane with enhanced water flux and salt selectivity [J]. Desalination, 2020, 493: 114661.

[49] Jiang Yanzhuang, Yang Qian, Zhang Lin, et al. Development of high-flux reverse osmosis membranes with MIL-101(Cr)/Fe3O4 interlayer [J]. Frontiers of Materials Science, 2024, 18(3): 240692.

[50] Choi W, Shin M, Lee G, et al. Anisotropic biofouling behavior of sharkskin-patterned desalination membranes [J]. Journal of Membrane Science, 2023, 683: 121814.

[51] Shang Wentao, Sun Feiyun, Jia Wei, et al. High-performance nanofiltration membrane structured with enhanced stripe nano-morphology [J]. Journal of Membrane Science, 2020, 600: 117852.

[52] Seyedpour S F, Dadashi Firouzjaei M, Rahimpour A, et al. Toward sustainable tackling of biofouling implications and improved performance of TFC FO membranes modified by Ag-MOF nanorods [J]. ACS Applied Materials & Interfaces, 2020, 12(34): 38285-38298.